

# Microstructured polymer optical fibre sensors for opto-acoustic endoscopy

Christian Broadway<sup>1</sup>, Daniel Gallego<sup>1</sup>, Andreas Pospori<sup>2</sup>, Michal Zubeł<sup>2</sup>, David J Webb<sup>2</sup>, Kate Sugden<sup>2</sup>, Guillermo Carpintero<sup>1</sup>, Horacio Lamela<sup>1</sup>

<sup>1</sup>Opto-Electronics and Laser Technology Group (GOTL), Universidad Carlos III de Madrid, <sup>2</sup>Aston Institute of Photonic Technologies, Aston University

## ABSTRACT

**Keywords:** Fibre Sensors, Polymer Optical Fibre, Endoscopy, Biomedical Applications, Opto-Acoustics

Opto-acoustic imaging is a growing field of research in recent years, providing functional imaging of physiological biomarkers, such as the oxygenation of haemoglobin. Piezo electric transducers are the industry standard detector for ultrasonics, but their limited bandwidth, susceptibility to electromagnetic interference and their inversely proportional sensitivity to size all affect the detector performance.

Sensors based on polymer optical fibres (POF) are immune to electromagnetic interference, have lower acoustic impedance and a reduced Young's Modulus compared to silica fibres. Furthermore, POF enables the possibility of a wideband sensor and a size appropriate to endoscopy. Micro-structured POF (mPOF) used in an interferometric detector has been shown to be an order of magnitude more sensitive than silica fibre at 1 MHz and 3 times more sensitive at 10 MHz.

We present the first opto-acoustic measurements obtained using a 4.7mm PMMA mPOF Bragg grating with a fibre diameter of 130  $\mu\text{m}$  and present the lateral directivity pattern of a PMMA mPOF FBG ultrasound sensor over a frequency range of 1-50 MHz. We discuss the impact of the pattern with respect to the targeted application and draw conclusions on how to mitigate the problems encountered.

## 1. INTRODUCTION

The field of opto-acoustics receives growing attention in the academic community, providing the functional analysis of physiological parameters and delivering relatively speckle free imaging with high optical contrast and high ultrasonic resolution [1]. The imaging depth of this technique is between several millimetres and a few centimetres in the 700-1700 nm region depending on the imaging resolution and the effective attenuation coefficient. The opto-acoustic effect begins with the emission of high energy laser pulses at a wavelength that will be absorbed by the target tissue or object. The incident light is absorbed by the target tissue, stimulating rapid thermo-elastic expansion and contraction. This expansion and contraction causes the emission of ultrasound over a wide frequency range; a typical opto-acoustic spectrum ranges from 100 kHz to 50 MHz. For this reason, detectors should be ultra-wideband in the frequency domain.

Opto-acoustic endoscopy harnesses the opto-acoustic effect to obtain functional information in a minimally invasive modality. Opto-acoustics enables concentration distribution imaging of chromophores such as haemoglobin oxygenation [2]. For this application the dimensions of the detector system are important as probes become more miniaturised for intravascular applications. Recent publications show endoscopic probe diameters ranging from 2.5 mm [3] down to 1.1 mm [4].

Piezo electric transducers are the industry standard for ultrasound detectors though these possess a number of limitations for opto-acoustics. Transducers have a sensitivity that is proportional to their size; offer a relatively limited bandwidth and are susceptible to electromagnetic interference [5]. These inherent issues are important factors when considering endoscopy.

Optical detection methods and in particular optical fibres present a customisable bandwidth, a typically small fibre diameter and an immunity to electromagnetic interference [6]. Optical detection schema include fibre Bragg gratings [7], Fabry-Perot cavities [8], interferometric fibre sensors [5] and micro-ring resonators [9].

\*cbroadwa@ing.uc3m.es; phone +34 624 8758; portal.uc3m.es/portal/page/portal/grupos\_investigacion/optoelectronics

Progressing towards opto-acoustic endoscopy, we have transitioned from interferometry to point detection with Bragg gratings, which offer high reflectivity and spectral customisation. Polymer optical fibres, Poly-Methyl-Methacrylate (PMMA) being the standard, demonstrate a number of mechanical properties that exceed those of silica optical fibres including a higher elastic limit and a much lower Young’s Modulus [6]. We have demonstrated in our work that micro-structured polymer optical fibres (mPOF) have an acoustic sensitivity over 9 times higher than a single mode silica counterpart over a 1-10 MHz range [10].

We have recently demonstrated the viability of a compact ultrasound point detector based on a PMMA mPOF Bragg grating over a 1-10 MHz range [6]. The next stage is to characterise the detector, assess its response and improve it by establishing the wider frequency response and the directivity of the detector.

We present the first opto-acoustic measurements obtained using polymer optical sensors. We present the lateral directivity of a PMMA mPOF FBG based detector over an incident frequency range of 1-50 MHz. We discuss the impact of the directivity pattern with respect to the targeted application and draw conclusions on how to mitigate the problems encountered.

## 2. EXPERIMENTAL SETUP AND METHODOLOGY

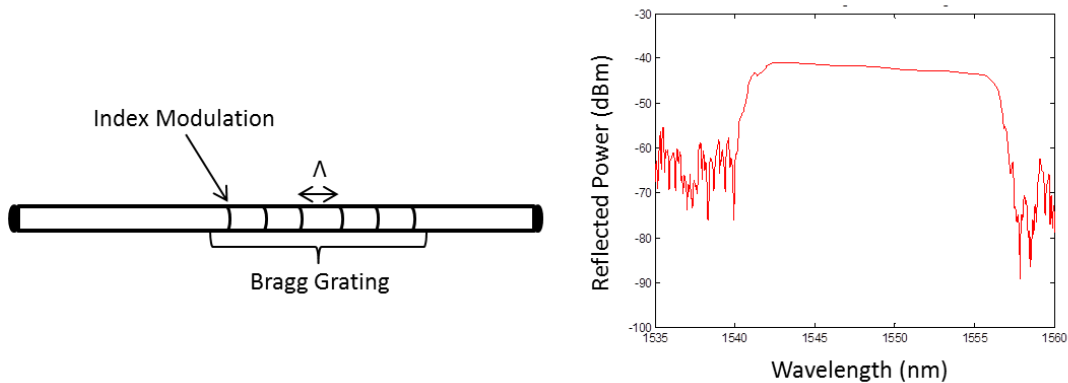


Figure 1. Fibre Bragg grating fundamental composition and a demonstration of its’ effect on the reflected spectrum from the fibre

A fibre Bragg grating (FBG) is a periodic modulation of the refractive index of the fibre core, producing a pass band in the reflected spectrum around a central wavelength, known as the Bragg wavelength. When the fibre is exposed to a number of stimuli such as varying strain, pressure and temperature, there is a corresponding shift in the refractive index of the fibre, causing a variation in the phase of the FBG profile itself. Depending on the material in question, optical fibres demonstrate different sensitivities to parameters; TOPAS is humidity insensitive while PMMA is highly humidity sensitive [11].

Ultrasonic emission is generated by opto-acoustically exciting a black painted PMMA block using an Nd:Yag laser, causing the paint layer to expand and contract, generating a plane wave ultrasonic response over a 1-50 MHz bandwidth. The laser emits pulses with a peak power of 50 mJ that are then expanded by a lens to illuminate the whole phantom. The detector is positioned 30mm from the phantom, as can be confirmed in figure 5A.

In our application, ultrasonic emissions induce a change in the grating profile that we monitor by converting it into a corresponding amplitude variation. This is achieved by tuning a laser to the 3 dB point of the FBG profile (see figure 2) and with the variance in amplitude recreates the incident ultrasonic pulse with a time delay equivalent to the distance of the sensor from the target.

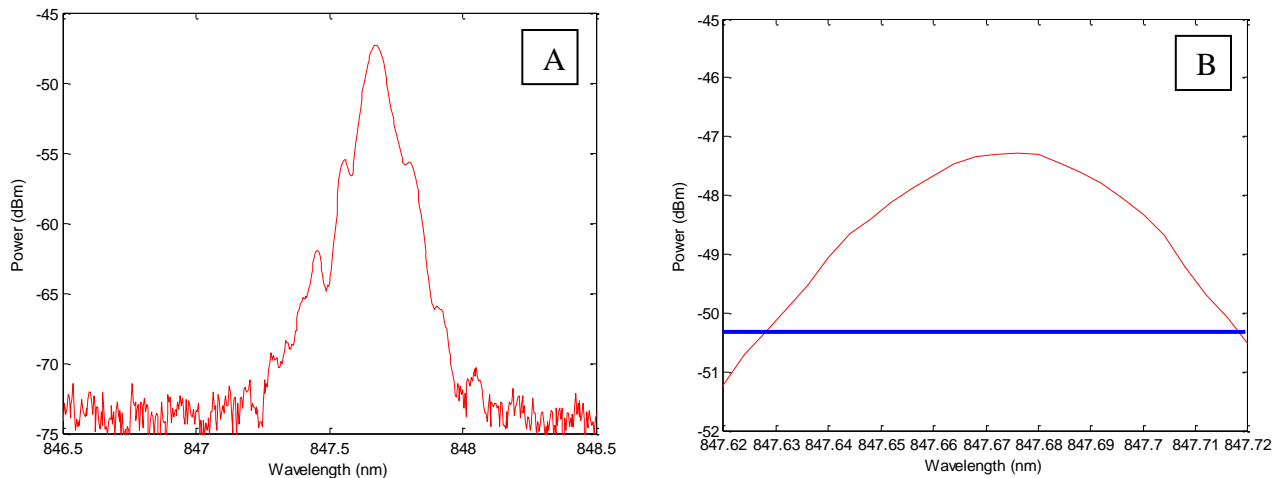


Figure 2. Reflected profile of the FBG (A) and profile showing the peak with the 3DB point demarcated by a blue line (B)

Having established the grating profile (see figure 2), we prepare the setup by establishing the angle and distance we will use with our calibrated sensor (WAT-13), a wideband piezo-electric transducer that has an active element with a 16 mm diameter and an acoustic range of 1 kPa to 10 MPa. We make the substitution for our calibrated sensor and immerse the fibre sensor in water, attached to a post that is secured in a 4 axis computer controlled positioning system of our own construction as shown in figure 4. We allow the spectral profile to stabilise, observing the change with an SLED (Exalos EXS210005-02) and an optical spectrum analyser (AQ6370B, Yokogawa). When the profile stabilises we replace these with an external cavity tuneable laser (Lion TEC-500, Sacher) and a photodiode (PDA10A, Thorlabs).

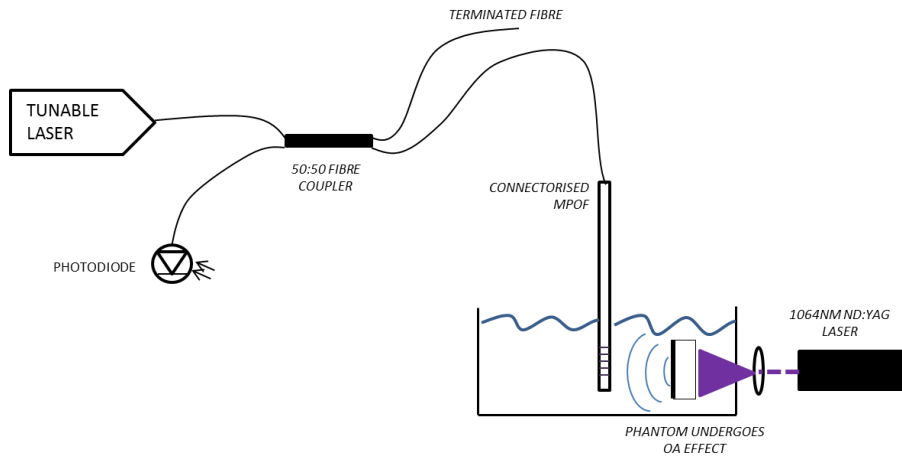


Figure 3. Detector schematic for opto-acoustic emission and detection

With the position and angle verified, we feed instructions to our positioning rig to produce the correct angles over a given range and record the opto-acoustic response every 0.5 degrees.

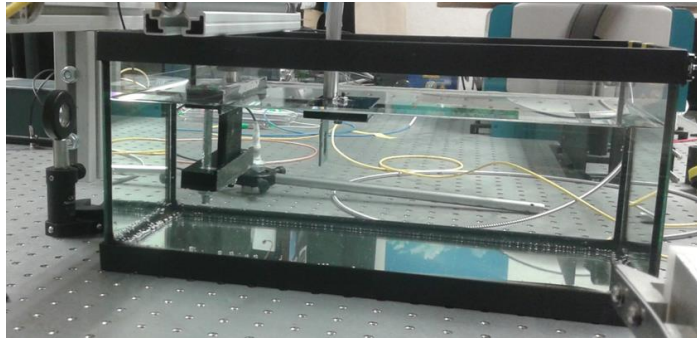


Figure 4. Photo of the setup with the black painted PMMA phantom and the mounted sensor suspended vertically on posts.

### 3. EXPERIMENTAL RESULTS AND DISCUSSION

We present the first opto-acoustic measurements obtained from POF, the sensor in question being a 4.7 mm Bragg grating inscribed into a 130  $\mu\text{m}$  diameter PMMA mPOF fibre. We compare these to our calibration sensor, specifically designed to provide a 100 MHz wideband response, as can be seen in figure 5D. We present the temporal and frequency spectra for both detectors and comment on the outcome.

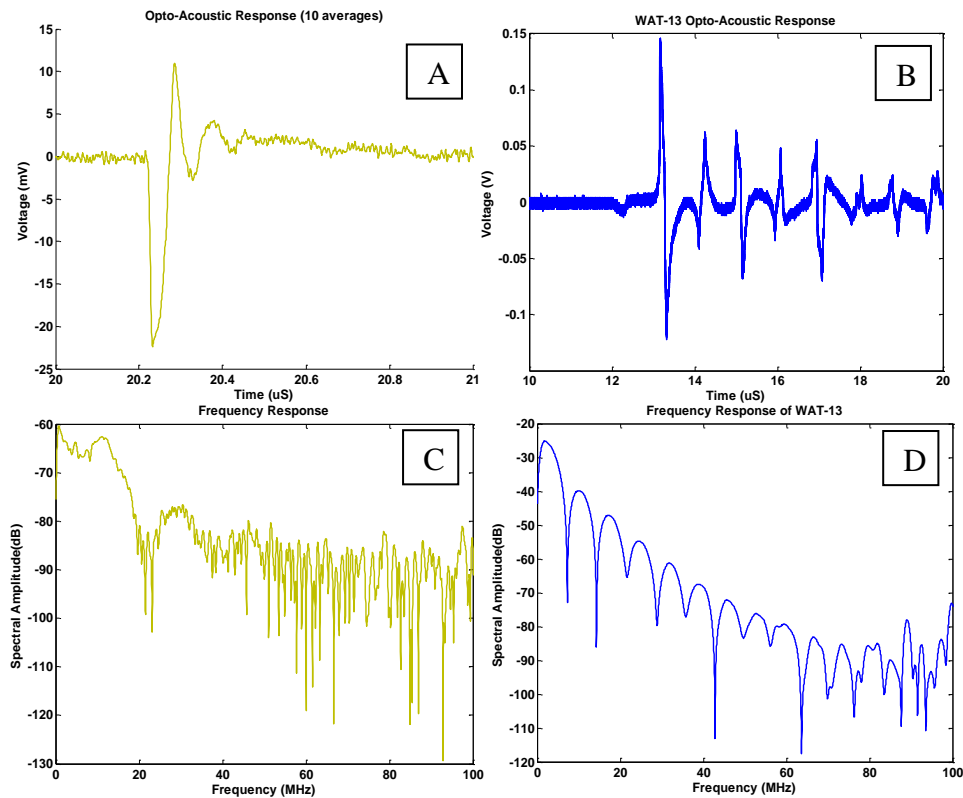


Figure 5. Opto-acoustic temporal response of our detector (A) compared to the opto-acoustic response of the WAT-13 transducer (B) and the frequency spectrum of each respective transducer (C and D)

We can observe a distinct pulse from the FBG that tends more towards the negative peak than the positive. We observe reverb 0.1  $\mu$ s after the primary pulse, indicating an additional 150  $\mu$ m distance travelled in water and therefore a point of origin 75  $\mu$ m beyond the sensor. Given that the fibre diameter is circa 130  $\mu$ m, the reverb can be reliably said to originate from the radial resonance of the fibre. Given the discrepancy in projected distance, it is worth noting that the mPOF geometry and construction provides an unknown speed for sound – PMMA provides a higher speed than water and air provides a much lower speed. Furthermore, the speed of sound changes as PMMA absorbs water. To investigate this further, it is essential to understand the speed of sound in mPOF for a given fibre geometry.

In the frequency domain (figure 5C) we observe a high frequency response in the 0 - 20 MHz region and a lower peak in the 20-30 MHz region. While the frequency response is low in general, this can be rectified by improving the detector performance in a number of ways to boost the output power such as an increased input power or a better photodiode.

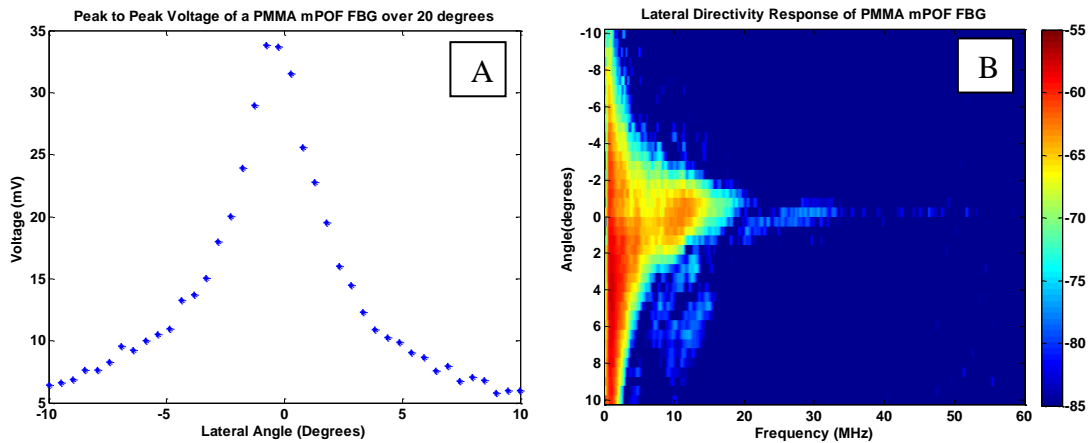


Figure 6. The change in voltage of the detector over a 20 degree angle (A) and the frequency directivity over the same window showing the power in decibels for each frequency (B)

The above directivity results show a perpendicular bandwidth of 20 MHz, 10 MHz that for an angle of  $\pm 2$  degrees, 5 MHz up to  $\pm 4$  degrees and a 2 MHz bandwidth over the remaining angles. We can observe that the directivity is stronger in general in the positive angles, giving rise to a number of possible causes that merit further investigation, seeking to establish the specific reasons for an asymmetric response and correcting them. Possible causes include bending in the fibre, imperfect fibre positioning relative to the centre of rotation, an uneven ultrasonic field, non-uniform fibre geometry and inhomogeneity caused by the effects of water absorption. These factors could all contribute towards the asymmetric lateral directivity. Returning to the application of endoscopy, these results are positive as they demonstrate a relatively narrow acceptance angle for signals laterally, meaning that the detector effectively scans a very small width azimuthally and will reduce the impact of other signals from outside the target area.

#### 4. CONCLUSIONS AND FUTURE WORK

We have presented the first opto-acoustic measurements obtained using polymer optical fibre sensors. We have also shown the lateral directivity of a PMMA mPOF FBG based detector over an incident frequency range of 1-50 MHz. We have shown that our detector has a 20 MHz bandwidth with a lateral directivity tolerance of plus or minus 2 degrees with a bandwidth of 10 MHz. We have concluded that to progress we need to examine ways to increase the signal to noise ratio and study the effects of the propagation of sound in mPOF fibres.

Our future work in the coming months comprises three sections. Firstly, we will complete the characterisation of the detector by analysing the azimuthal directivity and boost the lateral directivity analysis to a 30 degree window. Secondly we intend to explore potential improvements to the detector, including; an increase in the input power of the laser or using a more sensitive photodiode with a smaller bandwidth than the present model. Looking at the sensor in particular, we intend to explore the use of other fibre sensors. This means a potential transition from uniform FBGs to Fabry-Perot cavities or Pi-shifted FBGs to deliver a narrower spectral profile. It also potentially means a change in fibre material from PMMA to CYTOP and TOPAS, both of which present discrete advantages over PMMA. These workstreams will provide a concrete detector configuration that can then be brought towards implementation in an endoscopic probe.

## ACKNOWLEDGEMENTS

The research leading to these results has received funding from the People Programme (Marie Curie Actions) of the European Union's Seventh Framework Programme FP7/2007-2013/ under REA grant agreement n° 608382.

We acknowledge and thank David Saez Rodriguez, who fabricated the PMMA fibres that were inscribed, connectorised, characterised and implemented in the detector system described in this paper.

## REFERENCES

- [1] L.H.V. Wang, Photoacoustic Imaging and Spectroscopy, 1<sup>st</sup> ed., Optical Science and Engineering Series (CRC Press, 2009)
- [2] H. F. Zhang, K. Maslov, M. Sivaramakrishnan, G. Stoica, and L. H. V. Wang, "Imaging of hemoglobin oxygen saturation variations in single vessels in vivo using photoacoustic microscopy," *Appl. Phys.Lett.*, vol. 90, no. 5, art. no. 053903, Jan. 2007
- [3] J.-M. Yang, C. Favazza, R. Chen, J. Yao, X. Cai, K. Maslov, Q. Zhou, K. K. Shung and L.H.V. Wang, "Simultaneous functional photoacoustic and ultrasonic endoscopy of internal organs in vivo," *Nature Medicine*, 18(8), 1297 (2012).
- [4] X. Bai, X. Gong, W. Hau, R. Lin, J. Zheng, C. Liu, C. Zeng, X. Zou, H. Zheng, L. Song, "Intravascular Optical-Resolution Photoacoustic Tomography with a 1.1 mm Diameter Catheter" 20 March 2014 (8<sup>th</sup> June 2015).  
<http://www.ncbi.nlm.nih.gov/pmc/articles/PMC3961364/pdf/pone.0092463.pdf>
- [5] H. Lamela, D. Gallego and A. Oraevsky, "Optoacoustic Imaging using fiber-optic interferometric sensors", *Optics Letters* 34(23), 3695-3697 (2009).
- [6] C. Broadway, D. Gallego, A. Pospori, M. Zubel, D. J. Webb, K. Sugden, G. Carpintero and H. Lamela, "A compact polymer optical fibre ultrasound detector", *Proc. SPIE 9708, Photons Plus Ultrasound: Imaging and Sensing 2016*, 970813 (15 March 2016)
- [7] Amir Rosenthal, Daniel Razansky, and Vasilis Ntziachristos, "High-sensitivity compact ultrasonic detector based on a pi-phase-shifted fiber Bragg grating," *Opt. Lett.* 36, 1833-1835 (2011)
- [8] Benjamin T. Cox and Paul C. Beard, "The frequency-dependent directivity of a planar fabry-perot polymer film ultrasound sensor", *IEEE Transactions on Ultrasonics, Ferroelectrics, and Frequency Control* (Volume:54, Issue: 2) 2007, ISSN 0885-3010
- [9] S.-L Chen, S.-W. Huang, T. Ling, S. Ashkenazi and L.J. Guo, "Polymer microring resonators for high-sensitivity and wideband photoacoustic imaging", *IEEE Transactions on Ultrasonics, Ferroelectrics, and Frequency Control* (Volume:56, Issue: 11) 2009, ISSN 0885-3010
- [10] D. Gallego, D. Saez Rodriguez, D. J. Webb, O. Bang and H. Lamela, "Interferometric microstructured polymer optical fiber ultrasound sensor for optoacoustic endoscopic imaging in biomedical applications", *Proc. of SPIE Vol. 9157* (2014)
- [11] W. Yuan, L. Khan, D. J. Webb, K. Kalli, H.K. Rasmussen, A. Stefani and O. Bang, "Humidity insensitive TOPAS polymer fiber Bragg grating sensor", *Optics Express/ Vol 19 No.20/ 26 September 2011*